Fe_3O_4@SA MNCs Synthesis, Characterization, and First-time Use in Hydrogen Production by $NaBH_4$ Hydrolysis

Adil Umaz[1*]

[1]Mardin Artuklu University, Department of Medical Laboratory, Mardin, 47100, Turkey

Abstract: Hydrogen is a clean energy carrier that will reduce dependence on fossil fuels and contribute to reducing the harmful effects on the environment resulting from using fossil fuels. Hydrogen is produced by the hydrolysis of sodium borohydride ($NaBH_4$), one of the chemical hydrides, using a catalyst. In this study, Fe_3O_4@Salicylic acid magnetic nano-catalyst (Fe_3O_4@SA MNCs) was synthesized using the co-precipitation technique. The structural, physical, and chemical properties of the produced Fe_3O_4@SA MNCs were characterized by FT-IR, XRD, VSM, SEM, and SEM-EDX methods. At room temperature, the effect on hydrogen production performance was examined in the amounts of Fe_3O_4@SA MNCs (10, 25, 50, 75, and 100 mg), NaOH (0, 10, 20, and 25 mg), and $NaBH_4$ (25, 50, 100, 150 and 200 mg). The highest hydrogen generation rates (HGR) were obtained using 10 mg Fe_3O_4@SA MNCs, 150 mg $NaBH_4$, and 0 mg NaOH at room temperature. The obtained HGR value was calculated as 400 mL g_{cat}^{-1}.min^{-1}. Fe_3O_4@SA MNCs were used for hydrogen production for the first time in this study. This study showed that Fe_3O_4@SA MNCs exhibit catalytic properties and are a promising, efficient catalyst in hydrogen production from $NaBH_4$.

Keywords: Fe_3O_4@SA, hydrogen production, magnetic nano-catalyst, $NaBH_4$

Submitted: September 4, 2023. **Accepted**: October 23, 2023.

Cite this: Umaz A. Fe3O4@SA MNCs Synthesis, Characterization, and First-time Use in Hydrogen Production by $NaBH_4$ Hydrolysis. JOTCSA. 2024;11(1):205-216.

DOI: https://doi.org/10.18596/jotcsa.1354766.

***Corresponding author.** E-mail: adilumaz@gmail.com

1. INTRODUCTION

Population growth and rising living standards of individuals cause an increase in energy consumption. The decrease in fossil fuel reserves makes fossil fuel-based energy unsustainable. At the same time, due to fossil fuels, which are the dominant energy source, the world is facing serious climate change. Although fossil fuel-based energy meets a large part of the global energy demand, it has undesirable negative effects on humanity and the environment, such as greenhouse gas emissions, global warming, acid rain, and poor air quality. In order to prevent these vital negativities, researchers have started to focus on the search for innovative, carbon-free, sustainable alternative energy without environmental negative effects (1,2).

At this critical point, hydrogen energy is referred to as the best possible promising energy alternative that is environmentally friendly, renewable, and sustainable. Considering the cost-effectiveness and reliability of hydrogen energy, it has the potential to solve many environmental problems. When hydrogen is used as a fuel, it is expressed as a zero pollution producer because it gives water as a by-product (no treatment required) along with its excellent efficiency in energy conversion. Hydrogen is the most common and most abundant element in the universe. Hydrogen is found in compounds with other elements, such as carbon and oxygen. With this, it is an excellent clean energy carrier after separation (3).

Hydrogen energy can be produced from a wide variety of primary energy sources using different substrates and technologies and then used as the main energy source. $NaBH_4$ is used in hydrogen production technologies for its advantages, such as non-flammability, stability, and non-toxicity. Also, the hydrolysis of $NaBH_4$ can be controlled by suitable catalysts. The hydrolysis of $NaBH_4$ is shown in Equation 1. The catalyst is used to control the hydrolysis of NaBH4 and achieve higher reaction rates. The hydrolysis of $NaBH_4$ using inexpensive and environmentally friendly catalysts has recently received more attention (4,5).

$$NaBH_4 + 4H_2O \rightarrow NaBO_2 + 4H_2 \quad (1)$$

Nanotechnology offers effective materials with special structural design and a wide range of potential applications in environmental remediation solutions. The term "Nano" means a particle with at least one size less than 100 nm. Its nanoscale dimensions make its physical, optical, magnetic, chemical, mechanical, electrical, and magnetic properties significantly different from related materials. The application of nanomaterials in catalysis has attracted great interest. Nano-catalysts uniquely have selectivity, reactivity, enormous surface areas, and extended catalytic efficiencies. Homogeneous and heterogeneous catalysis applications are an evolving field. Excellent efficiency, highly selective, and fast catalytic systems are being developed through a green process. Research on environmentally friendly catalysis contributes to alleviating the pollution problem. Researchers continue to seek to obtain the ideal nano-catalyst with excellent stability, selectivity, and activity by green methods (6).

In nano-catalyst research, Fe_3O_4 with magnetic properties attracts great attention due to its attractive properties, such as low cost, easy preparation, easy modification, superparamagnetism, and non-toxicity (7). Fe_3O_4 consists of a magnetic core and has a good surface area/volume ratio. Fe_3O_4 has a high affinity, and a surfactant is often needed to both cause internal steric repulsion and modify its surface. Extensive studies have been carried out in various engineering applications with Fe_3O_4, whose surface is functionalized with appropriate functional groups (due to its optical, magnetic, electrical, catalytic, etc. properties) (8). Zero-valent metal nanoparticles supported on the bare surface of magnetite show reduced catalytic activity from incorporating iron into redox processes. Therefore, Fe_3O_4 needs to be coated with materials such as polymer, carbon, silica, etc. to support metal nanoparticles. Magnetically supported catalysts are considered promising materials with high activity and reusability due to their easy separation by an external magnetic field (9,10). Salicylic acid, which has phenolic, benzoic, carboxylic, and hydroxyl characters as functional groups, adds a very high potential to catalytic activity due to its intramolecular H-H bond structures (11). Because salicylic acid is o-hydroxybenzoic acid, it has π electrons that belong to aromatic compounds and are produced by orbital overlap. Thus, salicylic acid is used in catalysis studies (12).

In this study, Fe_3O_4@SA MNCs were produced for hydrogen production from $NaBH_4$. Fe_3O_4@SA MNCs were used for hydrogen production for the first time in this study. The catalytic activity of the synthesized magnetic nano-catalyst regarding hydrogen production by NaBH4 hydrolysis was investigated. Hydrogen production from hydrolysis of $NaBH_4$ of Fe_3O_4@SA MNCs with different parameters in experimental sets was investigated. SEM-EDX, XRD, VSM, and FT-IR analyses were performed to determine the morphological and structural characterization of Fe_3O_4@SA MNCs.

2. EXPERIMENTAL

2.1. Chemicals and Solutions

All chemicals and solvents used in the reactions are of analytical purity. Iron (III) chloride hexahydrate ($FeCl_3.6H_2O$, 99.9%) and salicylic acid ($C_7H_6O_3$, 99%) were purchased from MERCK Chemical. Iron (II) chloride tetrahydrate ($FeCl_2$ $4H_2O$, 98%) was purchased from Alfa Aesar Chemical Company. In addition, Ammonia (NH_3, 28.0%) and ethanol (CH_3CH_2OH, 99.9%) were purchased from ISOLAB.

2.2. Fe_3O_4@SA MNCs Synthesis

$FeCl_3.6H_2O$ (12 mmol) and $FeCl_2.4H_2O$ (6 mmol) were mixed in 200 mL of pure water in a two-neck flask at room temperature for 30 minutes. The temperature of the system was increased to 70 °C. For co-precipitation, 50 mL of 8 M NH_3 was added to the solution (The solution was orange at first but turned black with the addition of NH_3). The resulting black magnetite (Fe_3O_4) nanoparticles were stirred for another 30 minutes. Salicylic acid (0.6 mmol) was then added to the reaction system, and the reaction was continued for 30 minutes at system temperature. After the mixture in the balloon was cooled, Fe_3O_4@SA MNCs were isolated from the environment with the help of a magnet. Fe_3O_4@SA MNCs were washed and dried (13,14). The MNCs synthesis scheme is shown in Figure 1.

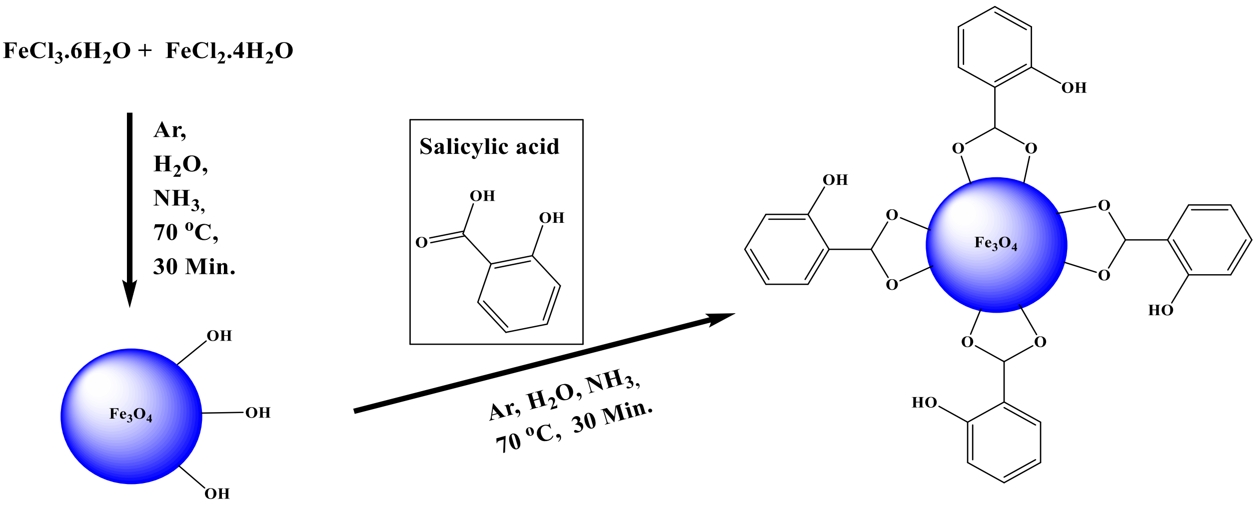

Figure 1. The synthesis scheme of Fe_3O_4@SA MNCs.

2.3. Characterization

It was done using Fourier transform infrared spectroscopy (FTIR) (Bruker Vertex 70, 4000-400 cm^{-1}) for identification of bonds in Fe_3O_4@SA MNCs structure, Vibrating Sample Magnetometer (VSM) for magnetization ability (Lake Shore 7407, -20000 – 20000 Oe), Scanning Electron Microscopy (SEM-EDX) (JEOL 6510) and X-ray Diffractometer (XRD) (Rigaku Smartlab).

2.4. Use of NaOH in Hydrogen Production

NaOH is generally used to inhibit the self-hydrolysis of $NaBH_4$. In this study, NaOH in amounts ranging from 0 to 25 mg was used to determine the effect of the amount of NaOH on hydrogen production.

2.5. Use of the Catalyst in Hydrogen Production

Fe_3O_4@SA MNCs in amounts ranging from 10 to 100 mg were used to determine the effect of catalyst amount on hydrogen production.

2.6. Hydrogen Production by $NaBH_4$ Hydrolysis

A round bottom reaction flask with a volume of 100 mL was utilized to introduce 150 mg of $NaBH_4$ and 10 mg of Fe_3O_4@SA MNCs. Following the addition of $NaBH_4$ and Fe_3O_4@SA MNCs, per the prescribed parameters, to the reaction flask at 25 °C, a volume of 20 mL of water was introduced. The solution was stirred at 500 rpm. The volume of hydrogen released was measured depending on time using the water-gas displacement method through an inverted gas cylinder filled with water. In this study, the effects of $NaBH_4$ (25, 50,100, 150 and 200 mg), NaOH (0, 10, 20, and 25 mg), and Fe_3O_4@SA MNCs (10, 25, 50, 75, and 100 mg) on hydrogen production were investigated. The HGR value was determined using the following formula (15,16).

$$HGR = \frac{mL\ H_2}{gram\ of\ catalyst \times time} \qquad (2)$$

In this formula, mL H_2, the volume of hydrogen produced, the amount of catalyst used and the time (min) was the reaction time were listed.

3. RESULTS AND DISCUSSION

3.1. Fe_3O_4@SA MNCs Characterization

In the FTIR spectrum of Fe_3O_4@SA MNCs, the peak at 545 cm^{-1} is the characteristic peak of the stretching of the Fe-O bond. The peak at 1610 cm^{-1} belongs to the C-O stretching vibration. The peak around 3000 cm^{-1} belongs to =C-H stretching vibrations. The peak around 3500 cm^{-1} belongs to the stretching of the O-H bond (Figure 2). The obtained peaks indicate that the synthesis of Fe_3O_4@SA MNCs has occurred successfully. The results obtained are compatible with the literature (17).

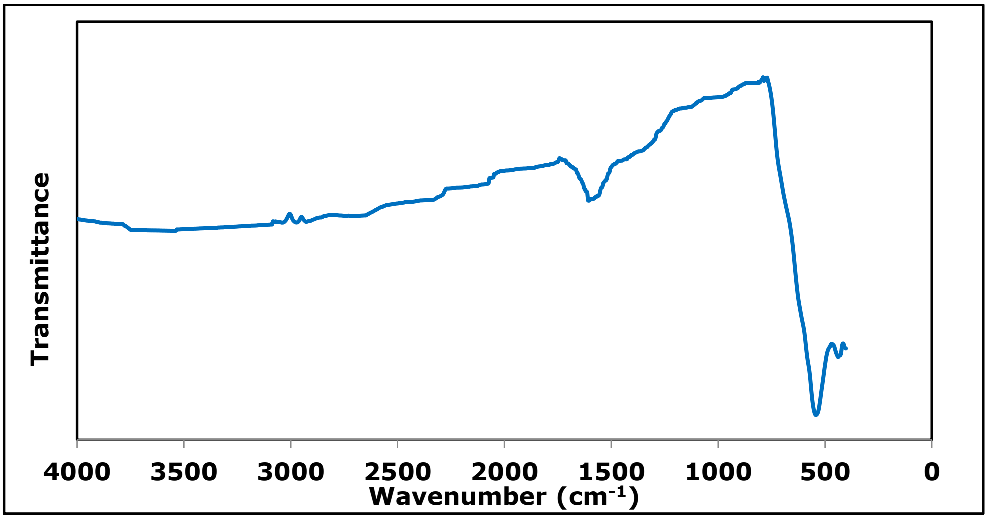

Figure 2. Fe_3O_4@SA MNCs FTIR spectrum.

Fe_3O_4@SA MNCs XRD patterns are given in Figure 3. Characteristic peaks at 2θ = 18.16°, 30.12°, 35.54°, 37.62°, 45.52°, 53.66°, 57.02°, 62.78° of Fe_3O_4@SA MNCs correspond to the crystal planes (1 1 1), (2 2 0), (3 1 1), (2 2 2), (4 0 0), (4 2 2), (5 1 1) and (4 4 0), respectively (Figure 3). The results show that Fe_3O_4@SA MNCs have a highly crystalline cubic spinel structure. The results obtained are compatible with the literature (18).

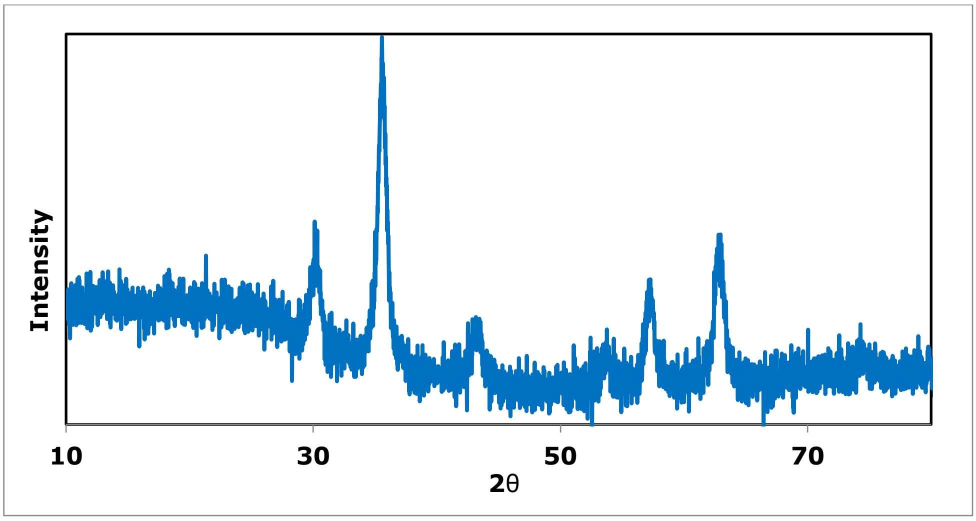

Figure 3: Fe_3O_4@SA MNCs XRD pattern.

The magnetic property of Fe_3O_4@SA MNCs is given in the VSM plot in Figure 4. Since hysteresis is not observed in the graph, it is understood that the sample is superparamagnetic. Saturation magnetic moment of Fe_3O_4@SA MNCs was found to be 52.8 emu/g (Figure 4). The high of this value indicates that Fe oxidation is either low or absent. The results obtained are compatible with the literature (19).

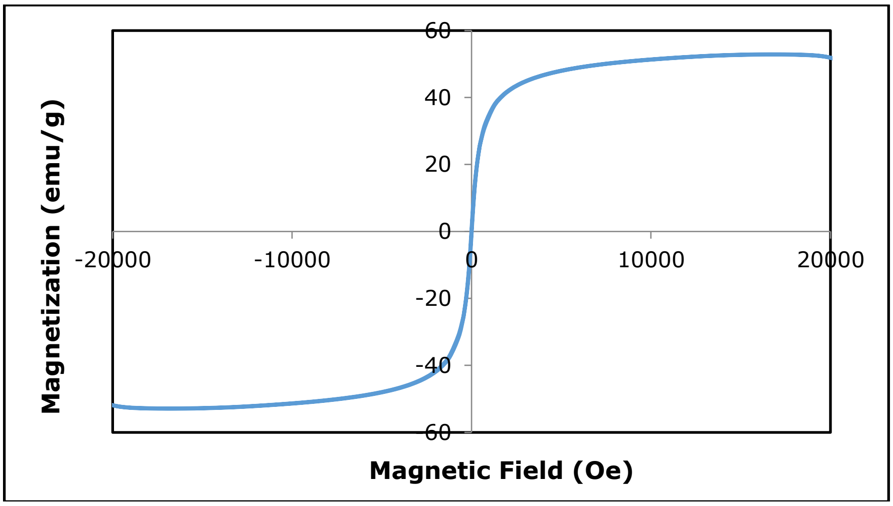

Figure 4: Fe_3O_4@SA MNCs VSM graphic.

Fe_3O_4@SA MNCs are given SEM images in Figure 5-A, SEM-EDS graph in Figure 5-B, and SEM-EDS-map graph in Figure 5-C. Figure 5-A shows that the morphology of Fe_3O_4@SA MNCs is spherical, spheres ranging in size from about 20 to 60 nm are adjacent to each other, and agglomeration is present. Its surface is rough. Figure 5-B shows that Fe_3O_4@SA MNCs, Fe (48.8%), O (33.1%), and C (18.1%) are formed. The obtained values show that the synthesis was successful. Figure 5-C demonstrates that the elemental distribution of Fe_3O_4@SA MNCs is very good. The results obtained are in accordance with the literature (18).

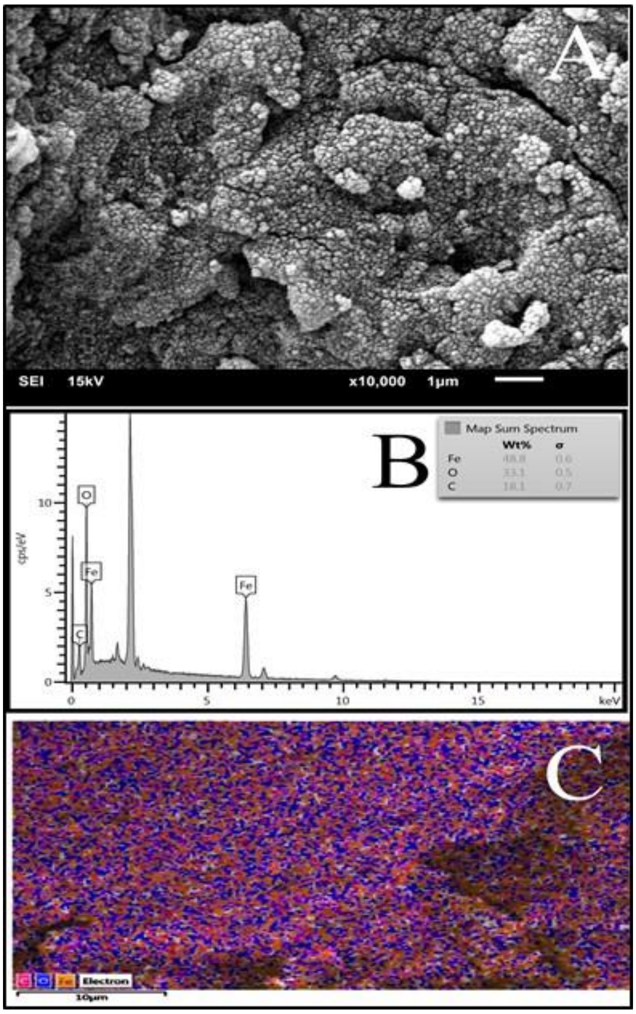

Figure 5: Fe_3O_4@SA MNCs A) SEM images, B) SEM-EDS graph, C) SEM-EDS-map graph.

3.2. $NaBH_4$ catalytic hydrolysis

3.2.1. Effect on hydrogen production of NaOH amount

To determine the appropriate amount of NaOH in the reaction solution, hydrogen productions were investigated using 50 mg Fe_3O_4@SA MNCs, 100 mg $NaBH_4$, and different amounts of NaOH (0, 10, 20, and 25 mg) at 25 °C. The resulting graph is shown in Figure 6. This graph illustrates a notable drop in the volume of hydrogen produced, from 84 mL to 12 mL, as the quantity of NaOH is augmented from 0 mg to 25 mg. The Fe_3O_4@SA MNCs exhibited optimal catalytic efficiency when NaOH was excluded from the solution. The best catalytic performance for the Fe_3O_4@SA MNCs used was achieved by not using NaOH in the solution, and the HGR value was 88 mL H_2 $gcat^{-1}\cdot min^{-1}$ was measured. It has been reported in the literature (20) that an increase in the amount of NaOH reduces the rate of hydrolysis. Using 10, 20, and 25 mg of NaOH, the HGR values were measured as 48, 16, and 12 mL H_2 $gcat^{-1}\cdot min^{-1}$, respectively. The decrease in the HGR value is related to blocking the active sites on the Fe_3O_4@SA MNCs of the NaOH increase.

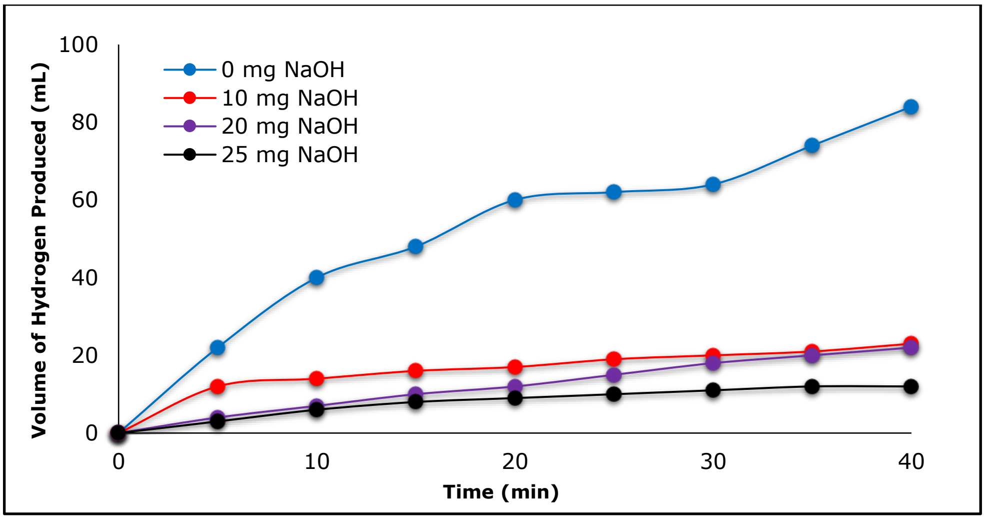

Figure 6: Effect on hydrogen volume in $NaBH_4$ hydrolysis of NaOH (Reaction conditions: 50 mg Fe_3O_4@SA MNCs, 100 mg $NaBH_4$, 0, 10, 20 and 25 mg NaOH and 25 °C).

3.2.2. Effect on hydrogen production of $NaBH_4$ amount

The effect on the hydrogen production of $NaBH_4$ was investigated by using 25, 50, 100, 150, and 200 mg $NaBH_4$ at 25°C, keeping the amount of Fe_3O_4@SA MNCs (50 mg) constant. Figure 7 shows that when $NaBH_4$ is increased from 25 mg to 200 mg, the hydrogen produced increases significantly from 50 mL to 314 mL. The best catalytic performance for the Fe_3O_4@SA MNCs used was achieved by using 200 mg of $NaBH_4$, and the HGR value was 157 mL H_2 $gcat^{-1}\cdot min^{-1}$ was measured. As the amount of $NaBH_4$ used increases, the hydrogen volume and HGR value increase depending on time. It was determined that as the amount of $NaBH_4$ increased, the hydrogen volume increased depending on time. The results obtained are compatible with the literature (21-23).

3.2.3. Effect on hydrogen production of catalyst amount

The effect on hydrogen production of Fe_3O_4@SA MNCs amount (10, 25, 50, 75, and 100 mg) in 150 mg $NaBH_4$ hydrolysis at 25 °C was investigated. The obtained graph is shown in Figure 8. When the amount of Fe_3O_4@SA MNCs increased from 10 mg to 75 mg, the hydrogen produced increased significantly from 106 to 128 mL. When the amount of catalyst increased from 75 mg to 100 mg, a significant decrease was observed in the volume of hydrogen produced. The reason for this decrease is that the catalyst's active sites are filled in the reaction and cannot provide enough active sites for the substrate. The results obtained are compatible with the literature (24).

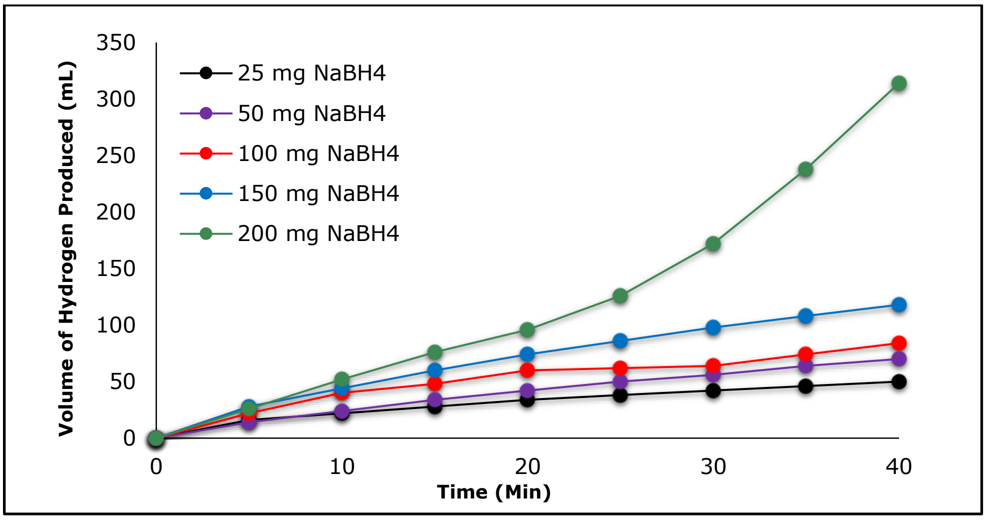

Figure 7: Effect on hydrogen volume of $NaBH_4$ using Fe_3O_4@SA MNCs (Reaction conditions: 50 mg nano-catalyst, 25, 50, 100, 150 and 200 mg $NaBH_4$ and 25 °C).

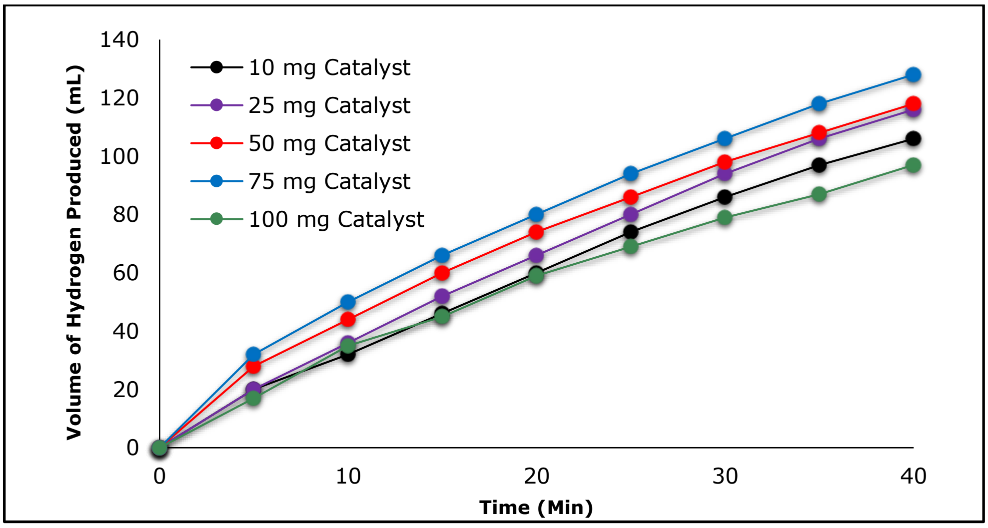

Figure 8: Effect on hydrogen volume by hydrolysis of NaBH4 of Fe_3O_4@SA MNCs (Reaction conditions: 10, 25, 50, 75, and 100 mg Fe_3O_4@SA MNCs, 150 mg $NaBH_4$ and 25 °C).

The best hydrogen production volume was achieved with 75 mg Fe_3O_4@SA MNCs, and the HGR value was measured as 85.33 mL H_2 $gcat^{-1}$·min^{-1}. The HGR values of 10, 25, 50, and 100 mg Fe_3O_4@SA MNCs were determined as 400, 160, 112, and 34 mL H_2 $gcat^{-1}$·min^{-1}, respectively. The highest HGR value was reached using a 10 mg catalyst. The HGR value increased until the optimum amount of Fe_3O_4@SA MNCs and then decreased. This is due to equation (2) used to calculate the HGR value.

Compared with Table 1, it was determined that the hydrolysis of $NaBH_4$ catalyzed by the Fe_3O_4@SA MNCs showed a lower HGR value than some catalysts, although it was comparable to other catalysts in the literature (Table 1). The reason for this can be said that the Fe_3O_4-supported structures in the literature have a more stable structure than the salicylic acid support material. Thus, higher HGR values can be obtained by coating the Fe_3O_4 structure with a more stable material and binding different metals to this nano-catalyst.

3.2.4. Reusability of the Fe_3O_4@SA MNCs

The percentage yield results obtained from $NaBH_4$ catalyzed after five reusability cycles of Fe_3O_4@SA MNCs at 25 °C are shown in Figure 9. It shows the yield results (percentage comparison with cycle 1) obtained from $NaBH_4$ catalyzed by Fe_3O_4@SA MNCs after five reusability cycles (75 mg catalyst, 150 mg $NaBH_4$, and 20 mL pure water) at 25 °C. As shown in Fig. 9, the catalytic activity of Fe_3O_4@SA MNCs was found to decrease slightly. It can be said that this situation is due to the accumulation of sodium metaborate, which cannot be removed by washing the catalyst. The results obtained are compatible with the literature (28). Thus, Fe_3O_4@SA MNCs were found to be an effective catalyst for the hydrolysis of $NaBH_4$.

Table 1. Comparison of Fe_3O_4@SA MNCs with various catalysts used for hydrogen production by $NaBH_4$ hydrolysis.

Catalyst	Temperature (°C)	HGR (mL H_2 $gcat^{-1}\cdot min^{-1}$)	Ref.
Co/Fe_3O_4@C	25	1403	(9).
Oxidized Fe_2O_3	25	264	(25).
α-Fe_2O_3@N-C NSs	25	637	(25).
Fe_3O_4@SiO_2–Pt	25	800	(26).
Fe_3O_4@SiO_2–Pt/Ni	25	2500	(26).
Fe_3O_4@SiO_2–Pt@TiO_2	25	1500	(26).
Fe-B	25	618	(27).
Fe_3O_4@SA	25	400	This work

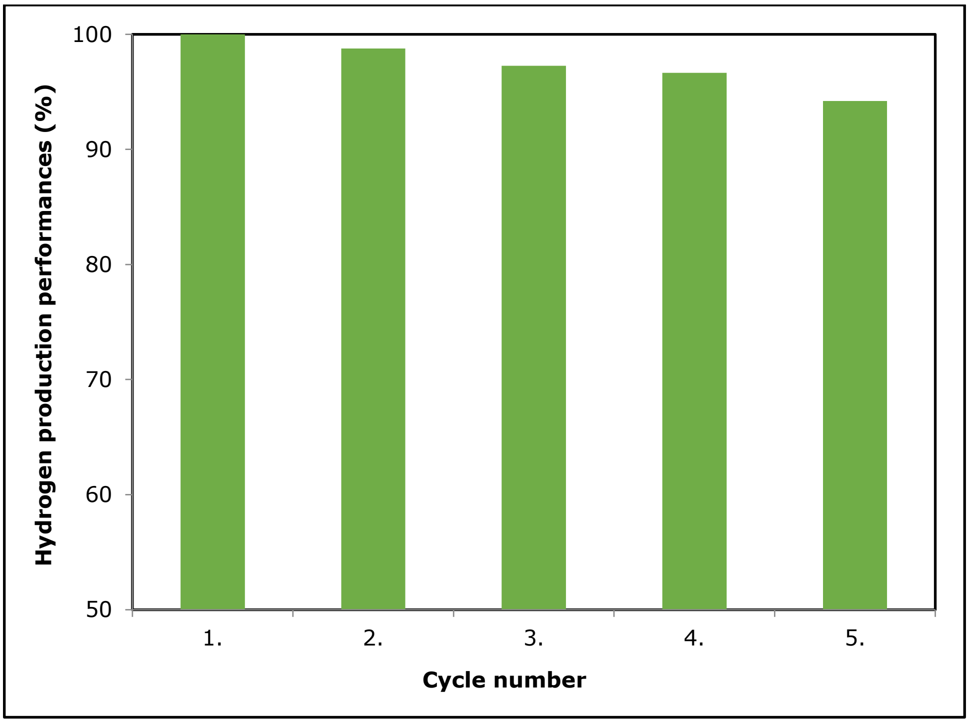

Figure 9: The reusability of Fe_3O_4@SA MNCs for hydrolysis of $NaBH_4$ at 25 °C.

3.3. Optimization of the Catalysis Process

In this study, optimum catalysis process conditions are given in Figure 9. The decrease in the amount of NaOH increased hydrogen production. The study with 0 mg NaOH produced 84 mL of hydrogen in 40 minutes, with other parameters remaining constant (Figure 9.A). Increasing the amount of $NaBH_4$ increased the hydrogen production. The study with 200 mg of $NaBH_4$ produced 314 mL of hydrogen in 40 minutes, with other parameters remaining constant (Figure 9.B). Increasing the amount of Fe_3O_4@SA MNCs increased hydrogen production. The study with 75 mg Fe_3O_4@SA produced 128 mL of hydrogen in 40 minutes, with other parameters remaining constant (Figure 9.C).

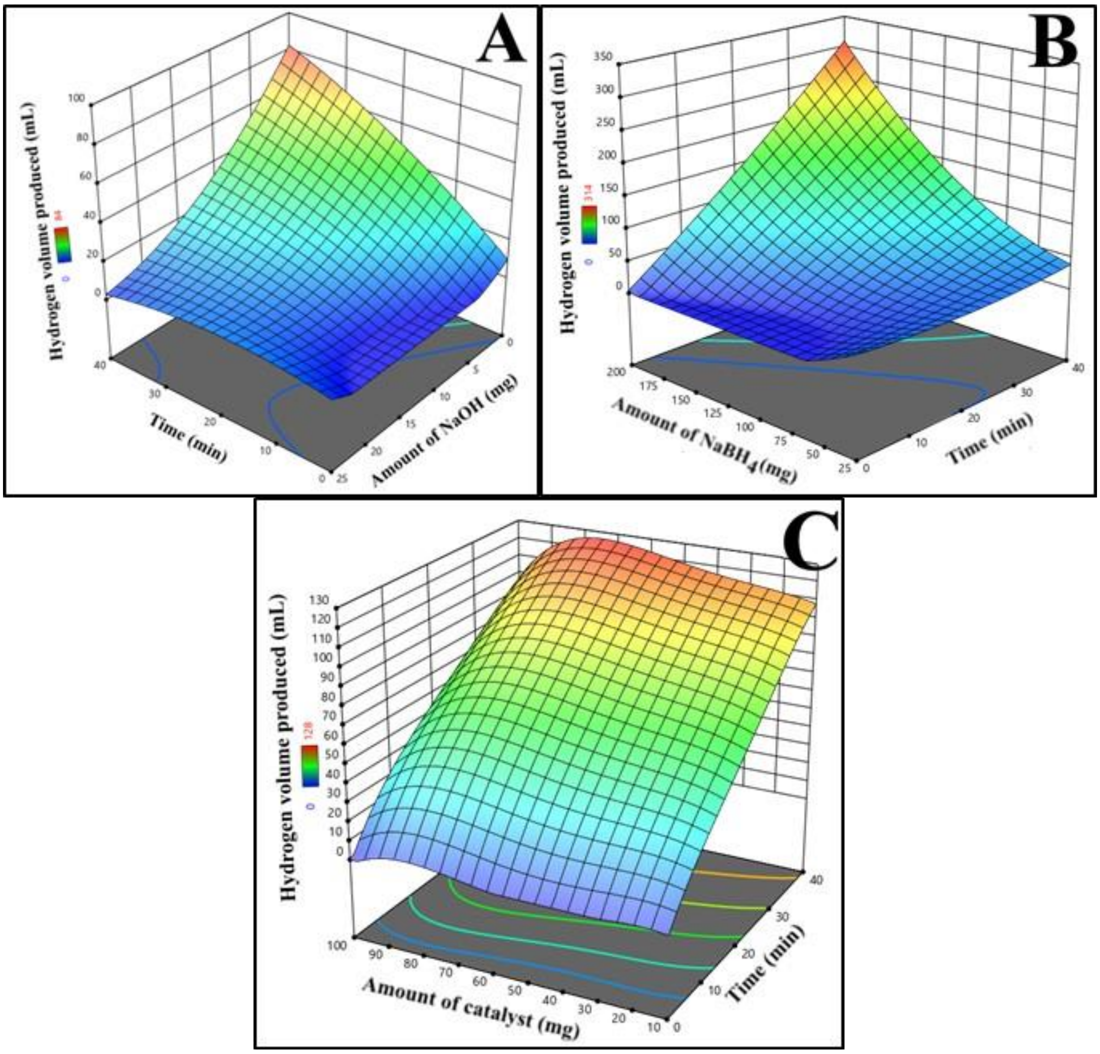

Figure 9: Optimization of the catalysis process A) NaOH amount-time graph, B) $NaBH_4$ amount-time graph, C) Fe_3O_4@SA MNCs amount-time graph.

3.4. A possible Mechanism of $NaBH_4$ Hydrolysis Catalyzed by Fe_3O_4@SA MNCs

The reaction mechanism of the catalyzed hydrolysis of $NaBH_4$ is assumed to occur by following the steps of the reaction mechanism, as shown in Figure 10. $NaBH_4$, catalyst, and water molecules are initially in the same environment. BH_4^- ions and water molecules are chemically adsorbed on the catalyst. Second, the H^- ion is transferred from the BH_4^- ion to the catalyst. Third, hydrogen in hydric form (H^-) and BH_3^- ions react with a water molecule to form H_2 and $BH_3(OH)^-$ ions. Hydrogen in each hydric form is transferred from the $BH_3(OH)^-$ ion to the catalyst. Finally, each cycle is repeated until 4 moles of H_2 are released, forming the $B(OH)_4^-$ form from the $BH_3(OH)^-$ ion. The proposed possible mechanism for $NaBH_4$ hydrolysis catalyzed by Fe_3O_4@SA MNCs is consistent with the literature (29,30). Since the reaction end product, $B(OH)_4^-$ is not supported by the catalyst, it reduces the rate of the hydrolysis reaction. It can be said that H_2 is produced more easily with the electrons coming from the BH_4^- ions from the hydrogen ion excess in the environment. Thus, it reflects positively on hydrogen production volume and HGR value.

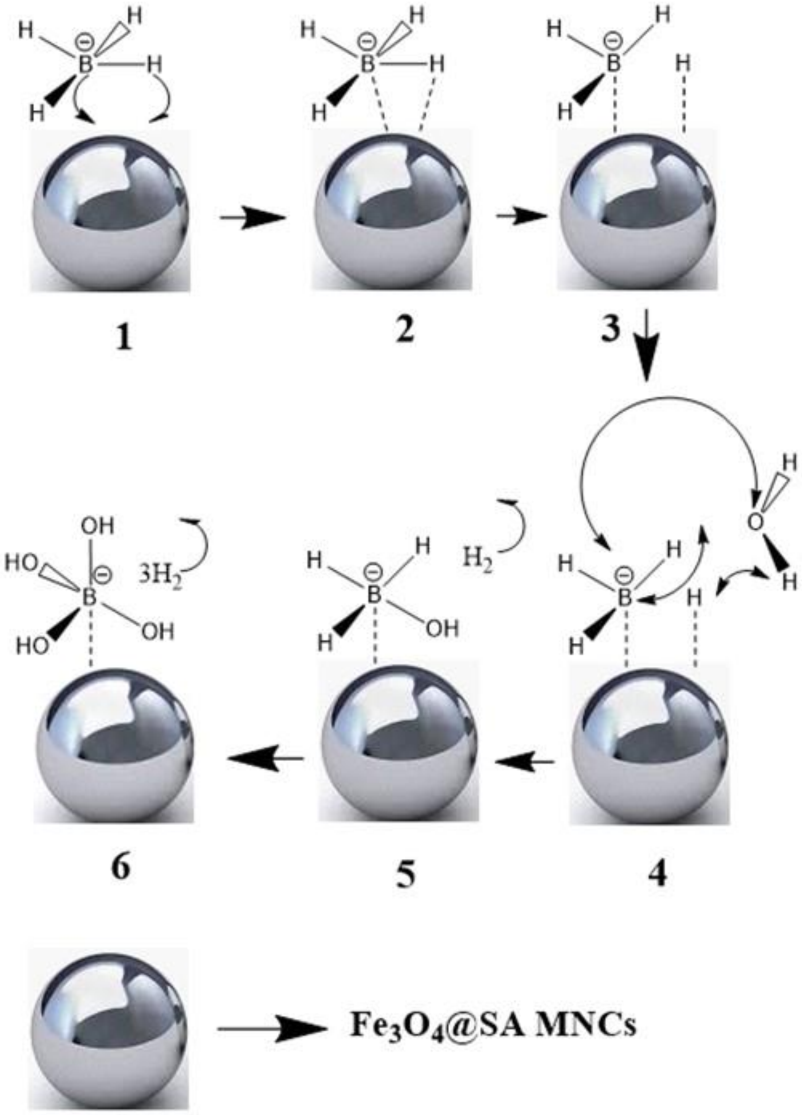

Figure 10: A possible mechanism of $NaBH_4$ hydrolysis catalyzed by Fe_3O_4@SA MNCs.

4. CONCLUSION

The use of Fe_3O_4@SA MNCs as a catalyst in hydrogen production was carried out for the first time in this study. Fe_3O_4@SA MNCs were produced by a simple, reliable, and inexpensive process. Characterizations with FT-IR, XRD, VSM, SEM, and SEM-EDX methods showed that Fe_3O_4@SA MNCs were successfully synthesized. To determine the effect of Fe_3O_4@SA MNCs on HGR, the amounts of $NaBH_4$, NaOH, and catalyst were examined. For Fe_3O_4@SA MNCs, the highest HGR value was obtained using 150 mg of $NaBH_4$, 10 mg of catalyst, 20 ml of distilled water, and no NaOH in the reaction. The obtained maximum HGR value is found as 400 mL H_2 $gcat^{-1} \cdot min^{-1}$. HGR values are comparable to values reported in the literature. The economic and large-scale production of Fe_3O_4-based magnetic nano-catalysts for hydrogen production by $NaBH_4$ hydrolysis offers a much simpler and more commercial process to make hydrogen the main fuel source.

5. CONFLICT OF INTEREST

The author declares that he has no conflicts of interest.

6. REFERENCES

1. Arsad A, Hannan M, Al-Shetwi AQ, Hossain M, Begum R, Ker PJ, et al. Hydrogen electrolyser for sustainable energy production: A bibliometric analysis and future directions. International Journal of Hydrogen Energy. 2023;48(13):4960-83. Available from: <URL>

2. Demirci S, Sunol AK, Sahiner N. Catalytic activity of amine functionalized titanium dioxide nanoparticles in methanolysis of sodium borohydride for hydrogen generation. Applied Catalysis B: Environmental. 2020;261:118242. Available from: <URL>

3. Sadiq I, Ali SA, Ahmad T. Graphene-based derivatives heterostructured catalytic systems for sustainable hydrogen energy via overall water splitting. Catalysts. 2023;13(1):109. Available from: <URL>

4. Bekirogullari M. Synthesis of waste eggshell-derived Au/Co/Zn/eggshell nanocomposites for efficient hydrogen production from NaBH4 methanolysis. International Journal of Hydrogen Energy. 2023. Available from: <URL>

5. Sahiner N, Ozay O, Inger E, Aktas N. Superabsorbent hydrogels for cobalt nanoparticle synthesis and hydrogen production from hydrolysis of sodium boron hydride. Applied Catalysis B: Environmental. 2011;102(1-2):201-6. Available from: <URL>

6. Agarwal N, Solanki VS, Pare B, Singh N, Jonnalagadda SB. Current trends in nanocatalysis for green chemistry and its applications-a mini-review. Current Opinion in Green and Sustainable Chemistry. 2023:100788. Available from: <URL>

7. Kutluay S, Ece MŞ, Şahin Ö, Kahraman Z, Ferat Ö, Fesih A. Derik Halhalı Zeytin Çekirdeğinden Çevre Dostu Selülozik Manyetik Nano-Adsorbent Üretimi ve Benzen Gideriminde Kullanılması. Bitlis Eren Üniversitesi Fen Bilimleri Dergisi. 2021;10(4):1535-51. Available from: <URL>

8. Ece MŞ. Fe3O4/AC@ SiO2@ EDTA Manyetik Nano-Adsorbentin Sentezlenmesi ve Toluenin Gaz Adsorpsiyonunda Kullanılması. Bitlis Eren Üniversitesi Fen Bilimleri Dergisi. 2020;9(2):561-72. Available from: <URL>

9. Chen B, Chen S, Bandal HA, Appiah-Ntiamoah R, Jadhav AR, Kim H. Cobalt nanoparticles supported on magnetic core-shell structured carbon as a highly efficient catalyst for hydrogen generation from NaBH4 hydrolysis. International Journal of Hydrogen Energy. 2018;43(19):9296-306. Available from: <URL>

10. Izgi MS, Ece MŞ, Kazici HÇk, Şahi̇n Ö, Onat E. Hydrogen production by using Ru nanoparticle decorated with Fe3O4@ SiO2–NH2 core-shell microspheres. International journal of hydrogen energy. 2020;45(55):30415-30. Available from: <URL>

11. Yang M, Xu A, Du H, Sun C, Li C. Removal of salicylic acid on perovskite-type oxide LaFeO3 catalyst in catalytic wet air oxidation process. Journal of hazardous materials. 2007;139(1):86-92. Available from: <URL>

12. Zhang P. Photocatalytic Reduction of Wo-3-Tio-2 Composite Catalyst in Cr (Ⅵ) Ion. International Journal of New Developments in Education. 2020;2(6). Available from: <DOI>

13. Ece MŞ. Synthesis, characterization and investigation of some physical textures of magnetite-silica-L-Proline nanoparticles modified with some transition metals (Co, Mn, Cu, Ni). Materials Science and Engineering: B. 2023;292:116417. Available from: <URL>

14. Kutluay S, Horoz S, Şahin Ö, Ekinci A, Ece MŞ. Highly improved solar cell efficiency of Mn-doped amine groups-functionalized magnetic Fe3O4@ SiO2 nanomaterial. International Journal of Energy Research. 2021;45(14):20176-85. Available from: <URL>

15. Wei Y, Wang M, Fu W, Wei L, Zhao X, Zhou X, et al. Highly active and durable catalyst for hydrogen generation by the NaBH4 hydrolysis reaction: CoWB/NF nanodendrite with an acicular array structure. Journal of alloys and compounds. 2020;836:155429. Available from: <URL>

16. Balbay A, Saka C. Semi-methanolysis reaction of potassium borohydride with phosphoric acid for effective hydrogen production. International Journal of Hydrogen Energy. 2018;43(46):21299-306. Available from: <URL>

17. Unal B, Durmus Z, Kavas H, Baykal A, Toprak M. Synthesis, conductivity and dielectric characterization of salicylic acid–Fe3O4 nanocomposite. Materials Chemistry and Physics. 2010;123(1):184-90. Available from: <URL>

18. Abdolmohammad-Zadeh H, Salimi A. A magnetic adsorbent based on salicylic acid-immobilized magnetite nano-particles for pre-concentration of Cd (II) ions. Frontiers of Chemical Science and Engineering. 2021;15:450-9. Available from: <URL>

19. Dheyab MA, Aziz AA, Jameel MS, Noqta OA, Khaniabadi PM, Mehrdel B. Simple rapid stabilization method through citric acid modification for magnetite nanoparticles. Scientific reports. 2020;10(1):10793. Available from: <URL>

20. Huang Y, Wang K, Cui L, Zhu W, Asiri AM, Sun X. Effective hydrolysis of sodium borohydride driven by self-supported cobalt oxide nanorod array for on-demand hydrogen generation. Catalysis Communications. 2016;87:94-7. Available from: <URL>

21. Yang L, Fan C, Zhang J, Zhang F, Li R, Yi S, et al. Poly (acrylic acid)-modified silica nanoparticles as a nonmetal catalyst for NaBH4 methanolysis. International Journal of Hydrogen Energy. 2021;46(45):23236-44. Available from: <URL>

22. Al-Enizi AM, Nafady A, El-Halwany M, Brooks RM, Abutaleb A, Yousef A. Electrospun carbon nanofiber-encapsulated NiS nanoparticles as an efficient catalyst for hydrogen production from hydrolysis of sodium borohydride. International Journal of Hydrogen Energy. 2019;44(39):21716-25. Available from: <URL>

23. Ghodke N, Rayaprol S, Bhoraskar S, Mathe V. Catalytic hydrolysis of sodium borohydride solution for hydrogen production using thermal plasma synthesized nickel nanoparticles. International Journal of Hydrogen Energy. 2020;45(33):16591-605. Available from: <URL>

24. Deonikar VG, Rathod PV, Pornea AM, Puguan JMC, Park K, Kim H. Hydrogen generation from catalytic hydrolysis of sodium borohydride by a Cu and Mo promoted Co catalyst. Journal of Industrial and Engineering Chemistry. 2020;86:167-77. Available from: <URL>

25. Nabid MR, Bide Y, Kamali B. Hydrogen release from sodium borohydride by Fe2O3@ nitrogen-doped carbon core-shell nanosheets as reasonable heterogeneous catalyst. International Journal of Hydrogen Energy. 2019;44(47):25662-70. Available from: <URL>

26. Ro G, Hwang DK, Kim Y. Hydrogen generation using Pt/Ni bimetallic nanoparticles supported on Fe3O4@ SiO2@ TiO2 multi-shell microspheres. Journal of Industrial and Engineering Chemistry. 2019;79:364-9. Available from: <URL>

27. Ocon JD, Tuan TN, Yi Y, de Leon RL, Lee JK, Lee J. Ultrafast and stable hydrogen generation from sodium borohydride in methanol and water over Fe–B

nanoparticles. Journal of power sources. 2013;243:444-50. Available from: <URL>

28. Hayagreevan C, Siva B, Rahul R, Denisdon S, Jeevagan J, Adinaveen T, et al. Sulphonated silica and sulphonated silica/carbon particles as efficient catalysts for hydrogen generation from sodium borohydride hydrolysis. International Journal of Hydrogen Energy. 2021;46(68):33849-63. Available from: <URL>

29. Zhang J, Li Y, Yang L, Zhang F, Li R, Dong H. Ruthenium nanosheets decorated cobalt foam for controllable hydrogen production from sodium borohydride hydrolysis. Catalysis Letters. 2022;152(5):1386-91. Available from: <URL>

30. Demirci UB, Miele P. Reaction mechanisms of the hydrolysis of sodium borohydride: A discussion focusing on cobalt-based catalysts. Comptes Rendus Chimie. 2014;17(7-8):707-16. Available from: <URL>